Neuron, Vol. 26, 331–343, May, 2000, Copyright ©2000 by Cell Press

Regulation of Presynaptic Terminal Organization by *C. elegans* RPM-1, a Putative Guanine Nucleotide Exchanger with a RING-H2 Finger Domain

Mei Zhen,*§ Xun Huang,*§ Bruce Bamber,† and Yishi Jin*‡
*Department of Biology
Sinsheimer Laboratories
University of California, Santa Cruz
Santa Cruz, California 95064
†Department of Biology
University of Utah
Salt Lake City, Utah 84112

Summary

Presynaptic terminals contain highly organized subcellular structures to facilitate neurotransmitter release. In *C. elegans*, the typical presynaptic terminal has an electron-dense active zone surrounded by synaptic vesicles. Loss-of-function mutations in the *rpm-1* gene result in abnormally structured presynaptic terminals in GABAergic neuromuscular junctions (NMJs), most often manifested as a single presynaptic terminal containing multiple active zones. The RPM-1 protein has an RCC1-like guanine nucleotide exchange factor (GEF) domain and a RING-H2 finger. RPM-1 is most similar to the *Drosophila* presynaptic protein Highwire (HIW) and the mammalian Myc binding protein Pam. RPM-1 is localized to the presynaptic region independent of synaptic vesicles and functions cell autonomously. The temperature-sensitive period of *rpm-1* coincides with the time of synaptogenesis. *rpm-1* may regulate the spatial arrangement, or restrict the formation, of presynaptic structures.

Introduction

Specialized subcellular structures at synatic junctions facilitate information flow between neurons and their target cells (Hall and Sanes, 1993; Burns and Augustine, 1995). At the presynaptic terminal, an electron-dense membrane structure, often called the presynaptic active zone, is surrounded by synaptic vesicles (Heuser and Reese, 1977; Landis et al., 1988; Hirokawa et al., 1989). The postsynaptic specialization also has distinct ultrastructural features and is rich in neurotransmitter receptors (Ziff, 1997; Sanes and Lichtman, 1999). Studies on different types of synapses have begun to elucidate the signaling cascades that regulate the formation of synaptic architecture.

At vertebrate cholinergic neuromuscular junctions (NMJs), agrin is released from the nerve terminals and acts through the MuSK receptor tyrosine kinase to coordinate the formation of pre- and postsynaptic subcellular specializations (for review, see Hall and Sanes, 1993; Sanes and Lichtman, 1999). At vertebrate central glutamatergic synapses and at *Drosophila* glutamatergic NMJs, the membrane-associated guanylate kinases (MAGUK), such as the vertebrate PSD-95/SAP90 (Cho et al., 1992; Kistner et al., 1993) and *Drosophila* Discs-large (DLG) (Woods and Bryant, 1991), are implicated in organizing the postsynaptic density (PSD) (for review, see Ziff, 1997; Gramates and Budnik, 1999). Ca^{2+}/calmodulin-dependent kinase II (CaMKII) and a Ras-GTPase-activating protein (SynGAP) form a macromolecular complex with MAGUKs and NMDA receptors (Kennedy et al., 1983; Chen et al., 1998; Kim et al., 1998). At the *Drosophila* NMJ, CaMKII regulates the synaptic localization of DLG and the morphology of the subsynaptic reticulum at the postsynaptic site (Koh et al., 1999).

Relatively few proteins are known to regulate the ultrastructural organization of presynaptic terminals. Electron microscopic (EM) studies of freeze-etched synapses revealed that synaptic vesicles are clustered at the presynaptic active zone and surrounded by a filamentous material that is mainly composed of actin and microtubules (Landis et al., 1988; Hirokawa et al., 1989). The phosphoprotein synapsins link synaptic vesicles to the presynaptic cytoskeleton and regulate synaptic vesicle maturation (Pieribone et al., 1995; Rosahl et al., 1995). Rim, a Rab3A effector protein, and Bassoon and Piccolo/Aczonin, identified from detergent-resistant synaptic membrane fractions of rodent brain extracts, are localized to the presynaptic active zone (Wang et al., 1997; tom Dieck et al., 1998; Wang et al., 1999; Fenster et al., 2000). All three proteins contain one to two zinc fingers and C2 domains. However, their in vivo functions are not known. The *Drosophila* DLG is also found in the presynaptic terminals of NMJs and controls the number of presynaptic active zones within a synaptic bouton by regulating the localization of the cell adhesion molecule Fasciclin II (Thomas et al., 1997).

The simple nervous system of *C. elegans* is well suited for studying synapse formation because the synaptic connectivity is known at the ultrastructural level, and individual synapses can be reliably identified based on their locations and ultrastructural morphology (White et al., 1976, 1986). Most of the presynaptic varicosities are filled with synaptic vesicles, and the presynaptic specialization has an electron-dense membrane structure that resembles those of some vertebrate central nervous system synapses. By contrast, *C. elegans* postsynaptic specializations often lack defined ultrastructural features. The *C. elegans* proteins that function in vesicle release and retrieval are also homologous in sequence and function to those in other organisms (Rand and Nonet, 1997).

Recently, a fluorescently tagged synaptic vesicle marker that is composed of a *C. elegans* synaptobrevin fused to the green fluorescent protein (SNB-1::GFP) has been used to visualize presynaptic regions in living animals (Chalfie et al., 1994; Hallam and Jin, 1998; Nonet, 1999). By recovering mutants that alter the expression of this marker, we identified a *C. elegans* Liprin gene,

‡To whom correspondence should be addressed (e-mail: jin@biology.ucsc.edu).
§These authors contributed equally to this work.

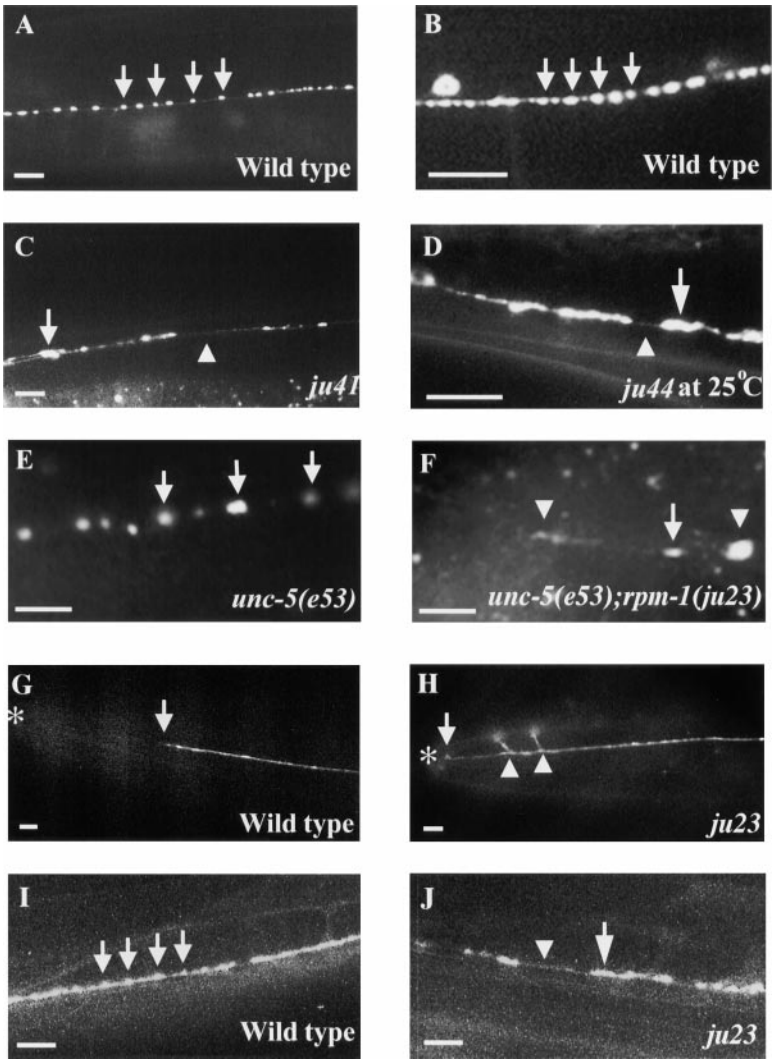

Figure 1. *rpm-1* Mutations Alter the Expression Pattern of Pre- and Postsynaptic Markers

(A–D) Expression of synaptic vesicle GFP marker in wild-type and *rpm-1* animals. Each GFP punctum (arrows) may represent an individual presynaptic terminal of DD (A and C) and VD (B and D) motor neurons, respectively. The GFP puncta in *rpm-1* animals are irregular in size; some (arrows) are larger than those in wild-type and are spaced unevenly, leaving gaps without GFP (arrowheads).

(E and F) SNT-1 expression in *unc-5(e53)* and *unc-5(e53); rpm-1(ju23)* animals. Arrows, wild-type SNT-1 puncta; arrowheads, abnormally shaped SNT-1 puncta.

(G and H) Axonal morphologies of ALM neuron in wild-type and *rpm-1* mutants, visualized by P_{mec-7}GFP. ALM process normally ends some distance (arrow) from the tip of the nose (star) but extends to the tip of the nose and has extra branches (arrowheads) in *rpm-1* mutants.

(I and J) Expression of UNC-49B::GFP in wild-type and *rpm-1* animals. *rpm-1* animals show uneven distribution of UNC-49B::GFP and contain large puncta (arrows) and gaps without GFP puncta (arrowheads).

Scale bars, 5 μm.

syd-2, that regulates the size of the electron-dense presynaptic active zones (Zhen and Jin, 1999). SYD-2 appears to be localized to or near the presynaptic active zone. We report here that loss-of-function mutations in the *rpm-1* gene (regulator of presynaptic morphology, originally named *syd-3* by us) result in abnormally structured presynaptic terminals in GABAergic NMJs. *rpm-1* encodes a protein that is homologous to *Drosophila* Highwire (HIW) and mammalian Pam. RPM-1 is localized to the presynaptic terminal and functions during synapse formation. Our results suggest that *rpm-1* signaling may regulate the distribution of presynaptic terminals or function to prevent the formation of excessive presynaptic structures.

Results

Mutations in *rpm-1* Alter the Distribution of Synaptic Vesicle Markers

C. elegans NMJs are formed en passant between the motor neuron processes and specialized branches of the muscle cells, called muscle arms (White et al., 1976, 1986). To visualize the presynaptic terminals of the GABAergic DD and VD motor neurons, we expressed the GFP-tagged synaptic vesicle marker under the promoter of the *C. elegans* glutamic acid decarboxylase gene *unc-25* (P_{unc-25}SNB-1::GFP, genotype designated *juIs1*) (Zhen and Jin, 1999). In wild-type animals, GFP is observed as distinct fluorescent puncta of 0.2–0.5 μm in diameter that are distributed evenly along the dorsal and ventral nerve cords (Figures 1A and 1B). The number and position of the fluorescent puncta are consistent with the distribution of GABAergic NMJs identified at the EM level (White et al., 1976; Jorgensen et al., 1995; Zhen and Jin, 1999).

Six alleles of the *rpm-1* gene (originally named *syd-3*) were isolated in a screen for abnormal presynaptic terminals using the P_{unc-25}SNB-1::GFP marker (see Experimental Procedures). Two additional alleles, *ky340* and *ky346*, were identified using a sensory neuron–specific marker (G. Crump and C. Bargmann, personal communication). All *rpm-1* mutations were recessive. In *rpm-1* mutants, the total number of the synaptic vesicle GFP puncta was reduced to various extents, and regions along the dorsal and ventral nerve cords often contained

no GFP puncta (Figures 1C and 1D). For example, in *rpm-1(ju23)* animals, there were 80 and 110 GFP puncta in the dorsal and ventral cords, respectively (n = 2), compared with 150 puncta in either the dorsal or ventral cords in wild-type animals (n = 2). The remaining GFP puncta were variable in size and shape (Figures 1C and 1D). The defects of the synaptic vesicle GFP marker were 100% penetrant, but the positions of abnormally shaped GFP puncta varied between individual animals, even among those of the same genotype. The mutant GFP puncta patterns in animals homozygous for *ju23*, *ju24*, *ju33*, *ju41*, and *ju48* were similar and did not show obvious differences from 15°C to 25°C. In these mutants, the abnormally shaped GFP puncta of the DD neurons were more severe than those of the VD neurons. Furthermore, the mutant phenotypes of homozygous *ju23* and *ju41* animals were less severe than those of *ju23/Df* and *ju41/Df* animals (data not shown), suggesting that these alleles are not null mutations.

rpm-1(ju44) homozygous animals displayed a temperature-sensitive mutant synaptic vesicle GFP pattern. At the permissive temperature (15°C), the number of fluorescent puncta was reduced to 80% of that in wild-type animals (120 puncta/dorsal cord in *ju44*, n = 2; 150 puncta/dorsal cord in wild type, n = 2), and the abnormally shaped fluorescent puncta were only seen at some presynaptic terminals of DD neurons. At the restrictive temperature (25°C), the total number of fluorescent puncta for both DD and VD neurons was reduced to more than half of that in wild-type animals (50 puncta/dorsal cord in *ju44*, n = 2; 150 puncta/dorsal cord in wild type, n = 2), and most of the remaining fluorescent puncta were abnormally large (Figure 1D). This temperature-sensitive phenotype of *ju44* was recessive because at 25°C, *ju44*/+ heterozygous animals exhibited normal GFP pattern. At 25°C, the defective GFP patterns in *ju44/Df* heterozygous animals and *ju44/ju44* homozygous animals were indistinguishable from each other. Moreover, the defective GFP patterns in *ju41/Df* and *ju41/ju44* at 25°C were also comparable, suggesting that *ju44* behaves as a genetic null mutation at 25°C. Thus, the mutant phenotype of *ju44* at 25°C may closely represent the null phenotype of *rpm-1*.

To determine if *rpm-1* mutations affected the distribution of other presynaptic components, we examined the expression of synaptotagmin (SNT-1) by immunocytochemistry. In wild-type animals, SNT-1 localizes to all neuronal presynaptic terminals (Nonet et al., 1993). At gross level, SNT-1 expression in *rpm-1(ju23)* animals looked similar to that in wild type (data not shown). The broad expression of SNT-1 precludes the analysis of its distribution at a single synapse. We therefore compared SNT-1 expression in the ectopic lateral NMJs of *unc-5* animals. *unc-5* encodes a netrin receptor (Leung-Hagesteijn et al., 1992). In *unc-5* mutants, the dorsal branches of some ventral cord motor neurons frequently fail to reach the dorsal cord and form NMJs at lateral positions. These ectopic NMJs are spaced apart along the body and have normal ultrastructure (Hedgecock et al., 1990). We found that SNT-1 expression at the ectopically formed NMJs in *unc-5(e53); rpm-1(ju23)* and *unc-5(e53); rpm-1(ju41)* animals resembled that of the synaptic vesicle GFP marker in *unc-5(e53); rpm-1(ju23)* animals; in particular, some SNT-1 puncta were larger than those in *unc-5(e53)* animals (Figures 1E and 1F). This observation suggests that the abnormal synaptic vesicle GFP expression in *rpm-1* mutants reflects an altered localization of endogenous presynaptic proteins.

The overall axonal morphology of most ventral cord motor neurons appeared normal, as examined by anti-GABA antibodies and GFP constructs (data not shown). However, we observed abnormal axonal morphologies in other types of neurons. For example, in *rpm-1(ju23)* animals, the anterior processes of the ALM mechanosensory neurons extended beyond their normal stopping positions and grew extra branches (64 of 74 *ju23* animals, compared with 6 of 59 wild-type animals) (Figures 1G and 1H). The nerve processes of three SAB motor neurons also frequently showed abnormal axonal trajectory (data not shown). At gross level, *rpm-1* mutant animals were slightly smaller than wild-type animals and displayed no abnormality in locomotion, egg laying, defecation, pharyngeal pumping, and male mating. In pharmacological assays, *rpm-1(ju24)* and *rpm-1(ju41)* animals showed the same sensitivity to aldicarb, an inhibitor for acetylcholinesterase, as wild-type animals (Nguyen et al., 1995) (data not shown), suggesting that cholinergic synaptic transmission is largely unaffected.

rpm-1 Mutations Also Affect the Distribution of Postsynaptic GABA Receptors

rpm-1 mutations were isolated based on altered patterns of a presynaptic marker. Studies of NMJs in *Drosophila* and vertebrates have shown that the differentiation of pre- and postsynaptic terminals is coupled (Gramates and Budnik, 1999; Sanes and Lichtman, 1999). We therefore asked if *rpm-1* mutations also affect postsynaptic components. The *C. elegans unc-49* gene produces several subunits of a heteromeric GABA receptor (Bamber et al., 1999). In wild-type animals, a functional GFP-tagged UNC-49 subunit, UNC-49B::GFP, was concentrated postsynaptically at GABAergic NMJs and appeared evenly distributed along the nerve cords (Figure 1I). In *rpm-1(ju23)* and *rpm-1(ju41)* animals, the UNC-49B::GFP fluorescent puncta were clustered in some regions, while absent in others along the nerve cords (Figure 1J). This altered UNC-49B::GFP pattern in *rpm-1* mutants resembles that of the synaptic vesicle GFP expression, suggesting a coordinated effect of *rpm-1* on the integrity of these NMJs.

The Abnormally Shaped Synaptic Vesicle GFP Puncta in *rpm-1* Mutants Contain Multiple Presynaptic Structures

Previously, we showed that a *C. elegans* Liprin protein, SYD-2, appears to be localized in or near the presynaptic active zones (Zhen and Jin, 1999). In immunocytochemical images of a wild-type GABAergic NMJ, one fluorescent punctum of SYD-2 protein is surrounded by a cluster of synaptic vesicles (Figure 2A). To further understand the synaptic defects in *rpm-1* mutants, we examined the coexpression pattern of SYD-2 and SNB-1::GFP at the DD and VD presynaptic terminals of *rpm-1(ju44*ts*)* raised at 25°C and of *rpm-1(ju23)* animals at 22.5°C (see Experimental Procedures). In these *rpm-1* mutants, the synaptic terminals that had normal shaped SNB-1::GFP puncta exhibited normal colocalization of SYD-2 and

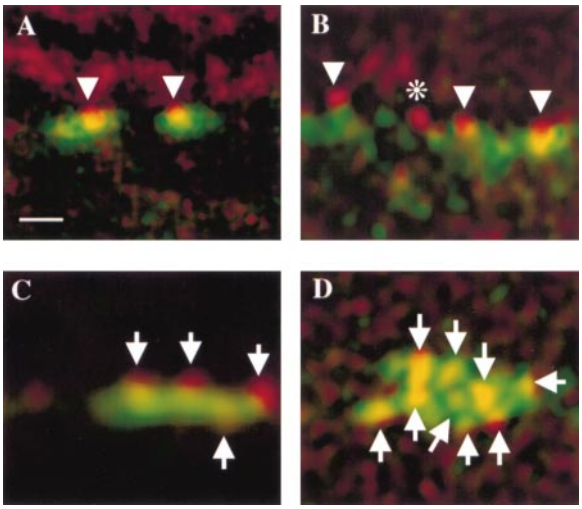

Figure 2. Abnormal SYD-2 Expression in the Presynaptic Terminals of GABAergic NMJs in *rpm-1* Mutants

Shown are superimposed confocal images of the immunofluorescent staining of SNB-1::GFP (green) and SYD-2 (red) at GABAergic NMJs; overlaps are yellow.

(A) Normal expression of SYD-2 and SNB-1::GFP at GABAergic NMJs in an animal of *syd-2(ju37) juIs330*[($P_{unc\text{-}25}$SYD-2(+)] *; juIs1* ($P_{unc\text{-}25}$SNB-1::GFP). *juIs330* rescues the defect of $P_{unc\text{-}25}$SNB-1::GFP in *syd-2(ju37)* (Zhen and Jin, 1999).

(B–D) Expression of SYD-2 and SNB-1::GFP in an animal of *rpm-1(ju41); syd-2(ju37) juIs330; juIs1*. Some SNB-1::GFP and SYD-2 puncta appear normal (arrowheads, [B]), some SNB-1::GFP puncta are larger and contain multiple SYD-2 puncta (arrows, [C and D]), and occasionally, SYD-2 is seen in the absence of SNB-1::GFP puncta (asterisk, [B]).

Scale bar, 500 nm.

SNB-1::GFP (Figure 2B). However, each abnormally shaped SNB-1::GFP punctum encompassed several closely positioned SYD-2 puncta (Figures 2C and 2D). In the synaptic terminal regions that lacked SNB-1::GFP, SYD-2 was mostly undetectable, although occasionally a SYD-2 punctum was found not associated with SNB-1::GFP (Figure 2B). These results suggest that the abnormally shaped SNB-1::GFP puncta in *rpm-1* mutants may represent a cluster of several presynaptic terminals and that the regions that lack SNB-1::GFP puncta may contain immature or defective presynaptic terminals.

To confirm the presynaptic defects in *rpm-1* mutants, we examined the morphology of GABAergic NMJs from electron micrographs of serial ultrathin sections. The presynaptic terminals of the wild-type GABAergic NMJs are seen as varicosities en passant along the axons at the interface between the muscles and the nerve cords. A typical presynaptic varicosity of GABAergic NMJs contains a single electron-dense presynaptic active zone that is surrounded by a few hundred synaptic vesicles 30–35 nm in diameter, along with a few large vesicles about 60 nm in diameter (Figures 3A and 3B; Table 1) (White et al., 1976, 1986). We analyzed the ultrastructure of GABAergic NMJs in *rpm-1(ju41)*, a strong loss-of-function mutation, and *rpm-1(ju44*ts*)* at 22.5°C (permissive temperature) and 25°C (nonpermissive temperature), in parallel with wild-type animals. Depending on the severity of the mutations, 30%–75% of the GABAergic NMJs from *rpm-1* mutants exhibited abnormalities in the presynaptic terminal morphology (Table 1). We categorized the ultrastructural defects into two classes: the "overdeveloped" class included those that contained more than two individual electron-dense presynaptic active zones within the same varicosity (Figures 3C and 3D); the "underdeveloped" class were those that had few synaptic vesicles and instead were filled with electron-dense debris-like material (Figures 3E and 3F). The presynaptic terminals with multiple active zones likely correspond to the abnormal synaptic vesicle GFP puncta that contain multiple SYD-2 puncta (Figures 2C and 2D), and those with few or no synaptic vesicles may correspond to the regions that lack the synaptic vesicle GFP puncta (Figures 1 and 2B). In wild-type GABAergic NMJs, each presynaptic terminal is surrounded by one to four muscle arms, and the electron-dense presynaptic active zone is positioned opposing only one of the muscle arms ($n = 24$). In *rpm-1* animals, the number of muscle arms at GABAergic NMJs was not affected; however, in the presynaptic terminals with multiple active zones, each active zone has docked vesicles and appears to oppose different muscle arms. The active zones in the presynaptic terminals with few vesicles were often less electron dense and less prominent.

rpm-1 mutations appear to have different effects on different types of synapses. In cholinergic NMJs, we found that in addition to the presynaptic terminals that contained electron-dense debris, some presynaptic terminals appeared to have a single active zone that spanned twice as many ultrathin sections as a typical cholinergic NMJ (Table 1) (360 nm for *rpm-1* mutants, $n = 3$; 120–180 nm for wild-type animals, $n = 20$). It is possible that the presynaptic terminals with longer active zones could represent a fusion of two or more neighboring presynaptic terminals. Synaptic vesicle GFP markers that label the presynaptic terminals of cholinergic motor neurons showed less severe abnormalities in their expression patterns than observed for GABAergic NMJs (data not shown). In synapses made between neurons, some presynaptic terminals contained electron-dense debris and few 30–35 nm synaptic vesicles (18 of 21 synapses in *ju41*; 6 of 10 synapses in *ju44* at 25°C; and 0 of 15 synapses in N2). We did not observe presynaptic terminals with multiple active zones at neuron–neuron synapses.

In summary, our phenotypic analyses at the light and EM levels reveal that different types of synapses are differentially affected by *rpm-1* mutations. At the GABAergic NMJs, the predominant mutant phenotype is a large presynaptic terminal containing multiple presynaptic active zones.

RPM-1 Is Highly Related to *Drosophila* HIW and Mammalian Pam

We mapped *rpm-1* between *dpy-11* and *unc-42* on chromosome V and rescued the Rpm-1 mutant synaptic vesicle GFP phenotype by germline transformation with cosmid C01B7 (Figure 4). The defects of the synaptic vesicle GFP puncta in *rpm-1* animals were fully rescued by genomic DNA clones containing the predicted gene, C01B7.6. Deletions and frameshift mutations of this predicted gene abolished the rescuing ability of transgenes

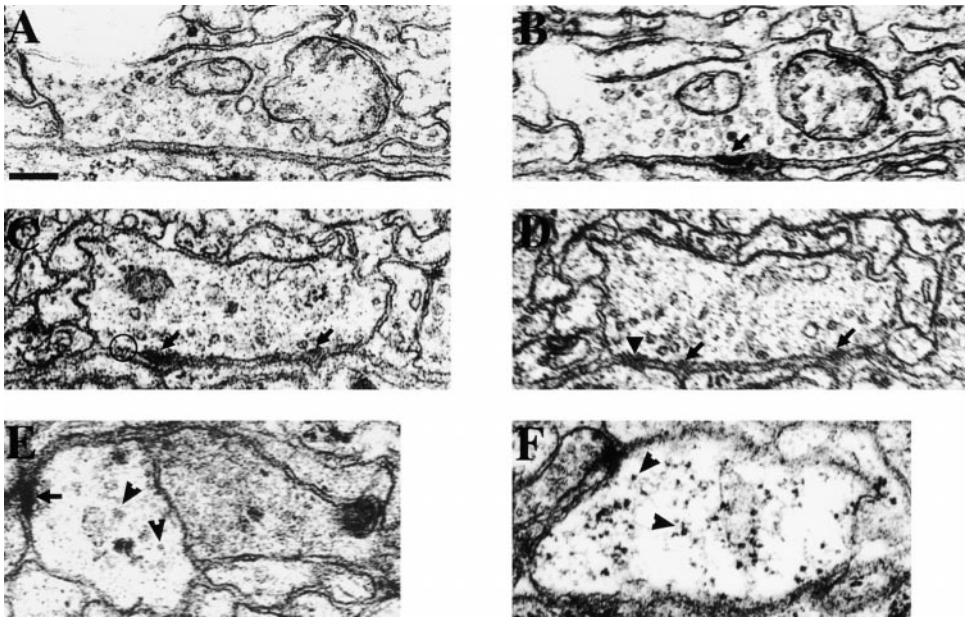

Figure 3. Abnormal Presynaptic Terminals in *rpm-1* Mutants

EM images of cross sections of the ventral nerve cord of wild-type and *rpm-1* mutant animals.

(A and B) Two adjacent sections of a GABAergic NMJ in a wild-type animal. Only one active zone exists in the presynaptic terminal (arrow, [B]).

(C and D) Two adjacent sections of a GABAergic NMJ in an *rpm-1(ju41)* animal. Two separate active zones are seen in both sections (arrows), and a third active zone appears at a new location (circle, [C]; arrowhead, [D]).

(E and F) Two presynaptic terminals with electron-dense debris (arrowheads) but few vesicles. Arrow (E), an active zone.

Scale bars, 200 nm.

(Figure 4). Moreover, we identified molecular lesions in several *rpm-1* mutants (see below), indicating that C01B7.6 corresponds to *rpm-1*.

The predicted RPM-1 protein is composed of 3766 amino acids and is highly similar in overall protein structure to the *Drosophila* protein HIW (Wan et al., 2000 [this issue of *Neuron*) and the mammalian protein Pam (Guo et al., 1998) (Figure 5A). HIW regulates the number of presynaptic boutons and the length of terminal arbor branches in *Drosophila* NMJs and localizes to presynaptic regions (Wan et al., 2000). Pam was identified as a nuclear protein that binds the Myc transcription-activating domain in tissue culture cells (Guo et al., 1998). All three proteins have a region at the N terminus that shows moderate similarity to the RCC1 (regulator of chromosome condensation) guanine nucleotide exchange factor (GEF) for the Ran GTPase (Bischoff and Ponstingl, 1991). RCC1 contains seven repeats, each of which contains 50–60 amino acids with several invariant Gly and His residues, and forms a seven bladed propeller-like structure (Renault et al., 1998). The RCC1-like region in RPM-1 resides between residues

Table 1. Quantitation of Presynaptic Ultrastructural Defects in *rpm-1* Mutants

Genotype	Type of NMJ	Single Active Zone and Normal Vesicles[a]	Multiple[b] or Longer[c] Active Zones	Vesicle Debris[d]
Wild type	GABAergic	23	1	0
	Cholinergic	25	0	0
rpm-1(ju41)	GABAergic	11	2	2
	Cholinergic	12	3	2
rpm-1(ju44) (22.5°C)	GABAergic	6	2	0
	Cholinergic	15	2	2
rpm-1(ju44) (25°C)	GABAergic	4	10	2
	Cholinergic	12	5	4

[a] Wild-type-like NMJs that contain numerous 30 nm vesicles and a single prominent active zone in the serial ultrathin EM sections spanning the synapse.

[b] GABAergic NMJs with more than one prominent active zone in the serial ultrathin EM sections spanning the synapse.

[c] Cholinergic NMJs in which a single active zone spans more sections than do those in wild-type.

[d] Presynaptic varicosities of NMJs that lack 30 nm vesicles but are filled with electron-dense debris. Such presynaptic terminals are unlikely to be artificial because they were observed in samples from different *rpm-1* mutants that were fixed independently and because from the same section, normal vesicles were present in different synapses.

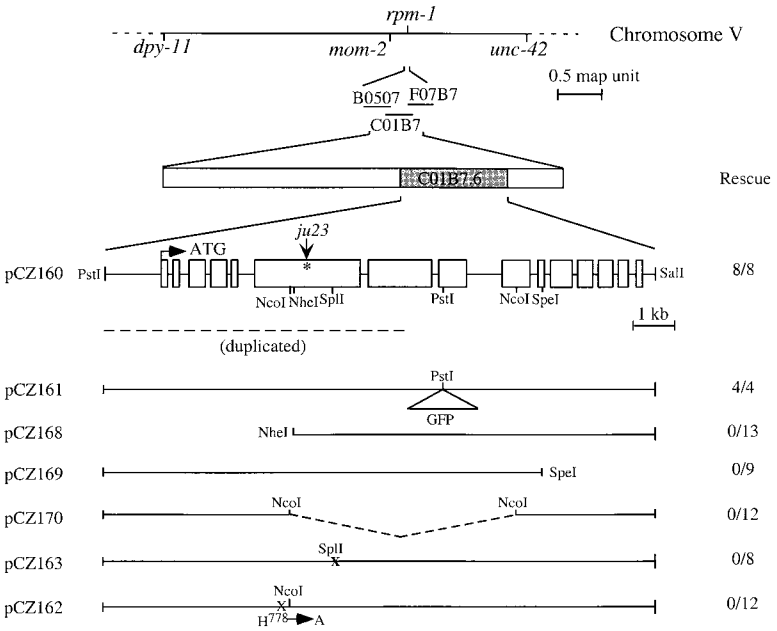

Figure 4. Cloning of *rpm-1*

rpm-1 corresponds to C01B7.6 (shaded boxes). The numbers on the right represent the number of transgenic lines that rescued *ju23* mutants out of the total number of lines. The dashed line below pCZ160 represents the duplicated region. Open boxes, exons; triangle, in-frame GFP insertion; dashed lines in pCZ170, deletion; x in pCZ163, fill-in at SplI.

452 to 892, among which repeats 4, 6, and 7 showed significant similarity with RCC1, and repeats 1, 2, 3, and 5 showed marginal similarity (Figure 5B). The highly conserved C terminus of the three proteins contains a B-box and a RING-H2 zinc finger (Borden and Freemont, 1996) (Figures 5A and 5C). All three proteins also have two repeats of 90 amino acids, which we name PHR repeats (for Pam/HIW/RPM-1) (Figure 5A). These repeats do not show significant similarity to known protein motifs in the database.

To understand how *rpm-1* mutations affect the function of the protein, we determined the molecular lesions in *rpm-1* alleles. Four strong mutations, *ju23*, *ju24*, *ju33*, and *ju41*, cause stop codon mutations at residues 950, 2634, 3321, and 3563, respectively (Figures 5A and 5C). Since *rpm-1* transgenes containing various truncations of the locus failed to rescue *rpm-1* (Figure 4; data not shown), the nonnull nature of these mutations may be due to the low level of full-length protein produced as the result of the readthrough. *ju44* alters a conserved cysteine (Cys-3675) to a tyrosine, and *ky346* alters a conserved arginine (Arg-3597) to a cysteine (Figure 5C). Both mutations are temperature sensitive. *ju44* behaves genetically as a null mutation at 25°C, suggesting that the C3675Y change in *ju44* may make the protein unstable at the restrictive temperature and result in a protein null mutant.

In the course of analyzing the DNA sequences from *rpm-1(ju23)* animals, we found that part of the *rpm-1* genomic locus has undergone a tandem duplication. Schaefer and colleagues made the same observation independently (Schaefer et al., 2000 [this issue of *Neuron*). The duplication includes the 9 kb 5′ genomic DNA of *rpm-1*, which includes the initiation Met to Ala-1952 (Figure 4; see Experimental Procedures). We addressed the role of this duplication in *rpm-1* function in the following experiments. First, we found that transgenes containing cosmid F07B7, which contains the duplication but not *rpm-1*, did not rescue *rpm-1(ju23)* (0 of 8 lines). Second, transgenes containing the duplicated genomic portion of *rpm-1* (pCZ169) failed to rescue *rpm-1(ju23)* (Figure 4) and did not cause any abnormality in wild-type animals (data not shown). Third, we examined the activity of transgenes containing a point mutation in the RCC1-like domain of RPM-1. Several conserved histidines in the RCC1 repeats have been shown to be crucial for GEF activity (Azuma et al., 1996). We mutated one such histidine (His-778) to alanine in the RCC1-like region of RPM-1 by site-directed mutagenesis (Figure 5B). The H778A mutation does not alter protein stability because transgenes carrying *rpm-1(H778A)::GFP* or *rpm-1::GFP* (pCZ161), in which GFP is inserted in-frame at Ala-2439 and does not affect *rpm-1* rescuing activity (Figure 4), showed equivalent levels of GFP expression (data not shown). We found that transgenes containing *rpm-1(H778A)* or *rpm-1(H778A)::GFP* were unable to rescue *rpm-1(ju23)* (Figure 4). Thus, our results suggest that the product from the duplication cannot replace or compensate for the function of RPM-1 and that the existence of this partial duplication does not affect our conclusions regarding the function and null phenotype of the *rpm-1* locus. Moreover, the H778A mutation study indicates that the RCC1-like GEF domain is required for RPM-1 function.

RPM-1 Is Localized to the Presynaptic Terminal Region

To determine how *rpm-1* might function, we examined its expression pattern using a functional RPM-1::GFP reporter transgene (pCZ161) and antibodies raised against the C-terminal 260 amino acids of RPM-1 (Figure 4; see Experimental Procedures). On whole-mount in situ preparations, the affinity-purified anti-RPM-1 antibodies detected weak expression of endogenous RPM-1 in the nerve ring, a synapse-rich region, in wild-type animals but not in *rpm-1(ju23)* and *rpm-1(ju44)* mutants (Figure 6A; data not shown). This weak expression could be due to low levels of endogenous RPM-1 protein or to

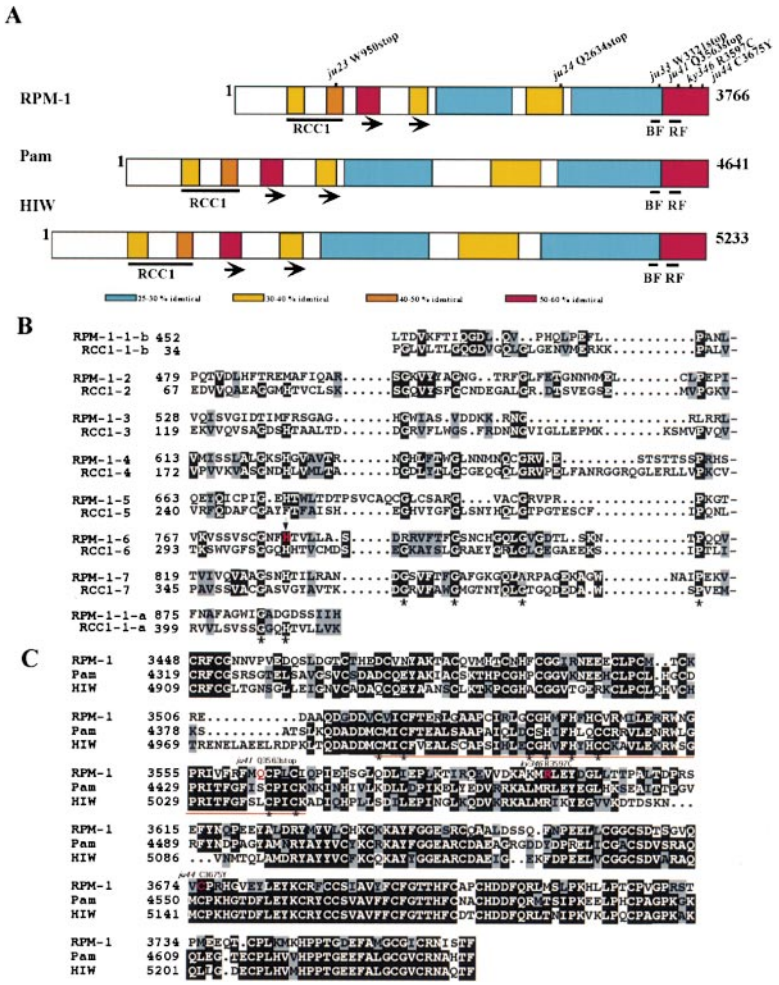

Figure 5. RPM-1 Protein and Mutant Lesions

(A) Comparison of RPM-1, Pam, and HIW. RCC1 and zinc finger domains are underlined, and the PHR repeats are represented by the arrows. The positions and molecular lesions of *rpm-1* alleles are indicated. Abbreviations: BF, B-box zinc finger; RF, RING-H2 zinc finger.

(B) Alignment of RPM-1 RCC1 repeats with human RCC1. Asterisk, conserved residues; arrow, His-778; dashes, interrupted sequences.

(C) Alignment of the C-terminal regions of RPM-1, Pam, and HIW. The RING-H2 finger is underlined.

low affinity of our anti-RPM-1 antibodies. In transgenic animals that overexpressed the functional RPM-1::GFP, both the anti-RPM-1 and anti-GFP antibodies gave identical patterns and showed that RPM-1::GFP was localized in distinct subcellular regions of the nervous system. Strong RPM-1::GFP expression was seen in the nerve ring and nerve cords (Figures 6B–6D) but not in commissural processes that do not form synapses. RPM-1::GFP expression was occasionally found in some neuronal cell bodies but was excluded from nuclei. Because we did not detect endogenous RPM-1 immunoreactivity in cell bodies, the presence of RPM-1::GFP at the cell bodies may be due to overexpression from the transgenes.

To assess the spatial distribution of RPM-1 with respect to other synaptic proteins, we costained the transgenic animals with anti-SNT-1 antibodies and anti-GFP antibodies. Analysis of confocal images revealed that RPM-1::GFP was localized adjacent to SNT-1 in presynaptic terminals (Figure 6E). We also coexpressed RPM-1 and SNB-1::GFP in the GABAergic DD and VD neurons specifically and found that RPM-1 and SNB-1::GFP were present in nonoverlapping regions at individual GABAergic NMJs (Figure 6F). This expression pattern suggested that RPM-1 was not associated with synaptic vesicles. Supporting this interpretation, we found that RPM-1::GFP localization was not changed in *unc-104* mutants, which are defective in synaptic vesicle transport (Hall and Hedgecock, 1991) (data not shown). Thus, we conclude that RPM-1 is localized to presynaptic regions independent of synaptic vesicles.

RPM-1 Functions Cell Autonomously in Presynaptic Neurons

rpm-1 mutants exhibit defects in both presynaptic structures and the localization of a postsynaptic marker. Although our expression studies did not reveal any expression of RPM-1 in muscle cells, we could not rule out the possibility that a very low level of RPM-1 may be present and function in postsynaptic cells. We performed two additional experiments to address whether *rpm-1* is required pre- or postsynaptically. First, we used the *unc-25* promoter to drive *rpm-1* expression specifically in VD and DD motor neurons in *rpm-1(ju23)* animals. This *unc-25* promoter is only active in the D neurons and in four RME cells (Jin et al., 1999). We observed a complete rescue of the abnormal patterns of both the presynaptic vesicle GFP marker and postsynaptic UNC-49B::GFP marker (data not shown). Second, we performed genetic mosaic analysis with *rpm-1(ju23)* animals carrying an extrachromosomal array containing the cosmid C01B7 and a cell-autonomous marker, SUR-5::GFP (Yochem

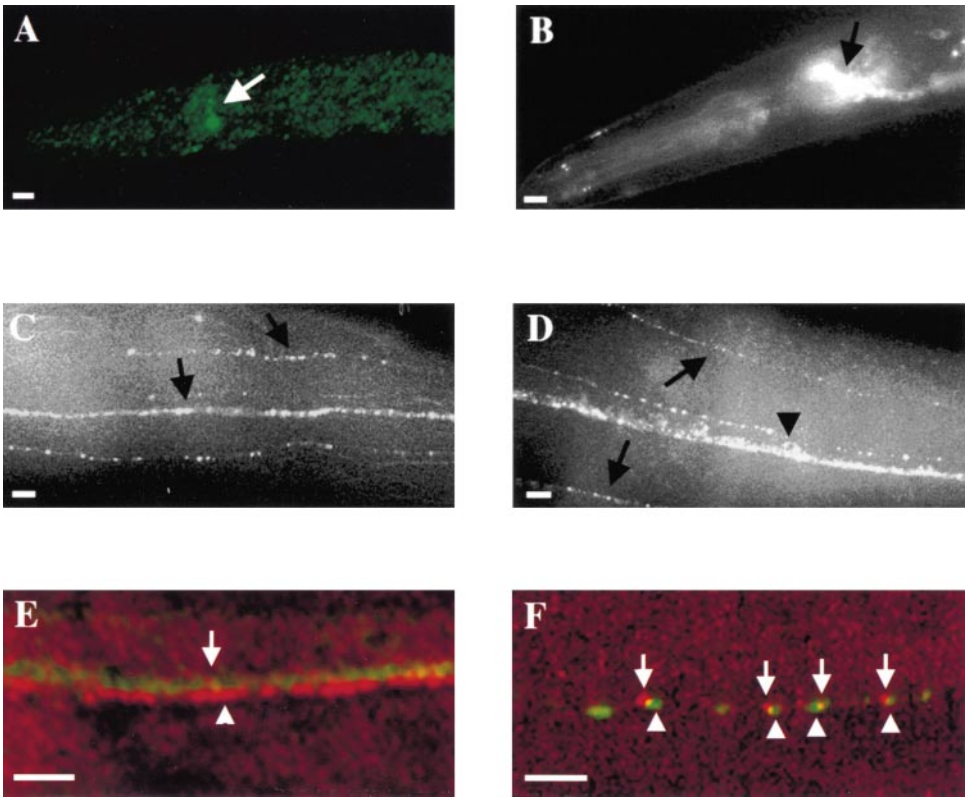

Figure 6. RPM-1::GFP Is Expressed in the Nervous System and Localized to Presynaptic Terminal

(A) Endogenous RPM-1 expression in the nerve ring (arrow) of a wild-type animal.

(B–D) Expression of RPM-1::GFP (*juIs58*), visualized by anti-GFP antibodies, in the nerve ring (arrow, [B]), the dorsal and subdorsal cords (arrows, [C]), and the ventral and subventral cords (arrows, [D]). Arrowhead, weak GFP expression in a ventral cord neuron cell body, excluding nuclei.

(E and F) RPM-1 is localized to presynaptic terminals but is not associated with synaptic vesicles. (E) shows a confocal image of the dorsal cord of *juIs58* animals costained with anti-GFP (green) and anti-SNT-1 antibodies (red). (F) shows GABAergic NMJs of transgenic animals carrying an extrachromosomal array of [$P_{unc\text{-}30}$SNB-1::GFP; $P_{unc\text{-}25}$RPM-1; pRF4] that are costained for RPM-1 (red) and SNB-1::GFP (green). Scale bars, 10 μm.

et al., 1998). All 13 mosaic animals that lost the *rpm-1(+)* array in neurons, but not in the muscles, had abnormal synaptic vesicle GFP puncta. By contrast, all 12 animals that lost the array in muscles, but not in neurons, showed a wild-type pattern of the synaptic vesicle GFP marker. These data indicate that RPM-1 functions presynaptically in a cell-autonomous manner. Moreover, the postsynaptic defect in the GABA receptor localization in *rpm-1* mutants is caused through a cross-talk originated from the neuron.

RPM-1 Is Required at the Time of Synaptogenesis

The defects in presynaptic structures in *rpm-1* animals could be caused by defects during the formation or maintenance of synapses. To address this question, we asked when *rpm-1* function was required for normal synapse morphology. The VD motor neurons are born at the end of the first larval (L1) stage, and their NMJs are made around the end of the L1 and early L2 stages (Sulston, 1976) (J. White, personal communication). The synaptic vesicle GFP expression pattern for the VD neurons in wild-type animals is the same at both 15°C and 25°C. In *rpm-1(ju44)* animals at the permissive temperature (15°C), the number of synaptic vesicle GFP puncta for VD neurons was slightly reduced (120 puncta/ventral cord in *ju44*, n = 2; 150 puncta/ventral cord in wild type, n = 2), but the puncta had normal shape nonetheless (Figure 7C). At the nonpermissive temperature (25°C), there was a great reduction in the number of GFP puncta (55 puncta/ventral cord in *ju44*, n = 2; 150 puncta/ventral cord in wild-type, n = 2), and 80% of these GFP puncta were abnormally large (Figure 7B). This temperature-sensitive phenotype is due to *rpm-1* because it was fully rescued by a wild-type *rpm-1* transgene introduced into *ju44* animals (data not shown). When *rpm-1(ju44)* animals grown at 15°C were shifted to 25°C before the L2 stage, the synaptic vesicle GFP puncta for the VD neurons were mostly abnormal. When *rpm-1(ju44)* animals grown at 25°C were shifted to 15°C before the L1–L2 stage, the synaptic vesicle GFP puncta for the VD neurons were mostly normal. Thus, both temperature upshift and downshift experiments identified an *rpm-1* temperature-sensitive period around the L2 stage (Figure 7A), which coincides with the period when VD neurons are born and form synapses. In wild-type animals, additional NMJs are added as worms grow from young

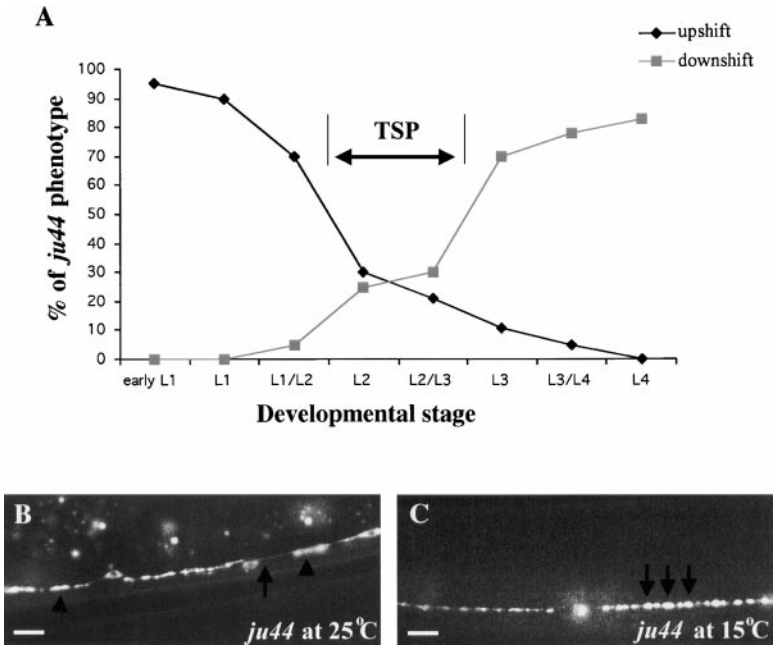

Figure 7. *rpm-1* Has a Temperature-Sensitive Period at the L2 Stage

(A) Graphic representation of temperature-sensitive period (TSP); x axis represents the developmental stages at which the upshift or downshift experiments were performed, y axis is the percentage of animals that showed *ju44* mutant GFP pattern.

(B and C) GFP pattern in *rpm-1(ju44)* at 25°C (mutant) and 15°C (mostly wild-type). Scale bars, 5 μm.

larvae to adults (Jorgensen and Rankin, 1997). It is currently unknown whether these later NMJs are formed de novo or by growing from existing NMJs. We observed no obvious changes in the shape and size of the synaptic vesicle GFP puncta in the same *rpm-1(ju44)* animal (shifted to 25°C from early L1) over a period of 3 days (L4 to 2-day-old adults, n = 15), suggesting that *rpm-1* does not affect synaptic addition during this growth period. Our data support a role of RPM-1 in the initial formation of presynaptic terminals.

Discussion

At presynaptic terminals, a large number of synaptic vesicles are clustered in an orderly fashion around electron-dense presynaptic active zones. How such specialized subcellular structures are formed is poorly understood. We have shown here that the *C. elegans rpm-1* regulates presynaptic terminal organization at GABAergic NMJs. Loss-of-function mutations in *rpm-1* result in abnormal presynaptic terminals that either contain multiple active zones or appear underdeveloped, with few synaptic vesicles. RPM-1 and the *Drosophila* HIW and the mammalian Pam define a new family of proteins. RPM-1 is localized to presynaptic terminal regions independent of synaptic vesicles and functions in neurons during NMJ formation. We propose that RPM-1 signaling may regulate the spatial arrangement of presynaptic terminals or restrict the development of presynaptic terminals.

Diverse Presynaptic Morphologies in *rpm-1* Mutants

rpm-1 mutations were isolated based on the abnormal morphologies of presynaptic terminals visualized by the synaptic vesicle–tagged GFP markers expressed in different types of neurons, hence the name regulator of presynaptic morphology (this work; Schaefer et al., 2000; G. Crump and C. Bargmann, personal communication). Our analysis of the GABAergic NMJs has revealed that loss of *rpm-1* function causes two types of defects: overdeveloped presynaptic terminals that contain multiple presynaptic active zones and underdeveloped presynaptic terminals that have few synaptic vesicles. In the strongest mutant background (*rpm-1(ju44)* at 25°C), both types of abnormality are present, and the overdeveloped presynaptic terminals appear to be predominant. Interestingly, part of the *rpm-1* locus is duplicated in the genome and is predicted to encode a protein that would contain the N-terminal half of RPM-1. It is possible that double mutants for both *rpm-1* and this duplication may have more severe defects than do *rpm-1* mutants alone, which remains to be determined. However, our transgenes, which mimic this partial duplication, did not rescue any of the defective synaptic vesicle GFP pattern in GABAergic NMJs of *rpm-1* mutants, suggesting that the duplication cannot functionally replace *rpm-1* during GABAergic NMJ formation.

rpm-1 is widely expressed in the nervous system. Different types of neurons appear to be affected in different manners and to different extents in *rpm-1* mutants. The defects in cholinergic NMJs are similar to, but less severe than, those of GABAergic NMJs, and the abnormal presynaptic terminals either contain few vesicles or have elongated presynaptic active zones. We observed no obvious axonal morphological defects in GABAergic and cholinergic motor neurons of the ventral nerve cord. By contrast, the axons of mechanosensory and SAB motor neurons have extra branches, often bypass their targets, and make few synapses (this work; Schaefer et al., 2000). It is not known whether the synapses of these mechanosensory and SAB neurons are affected at the ultrastructural level. Such "bypass" phenotypes could be caused by a failure in recognizing targets or could be a secondary effect of failures in the initiation and stabilization of synapse formation. Formation of NMJs

between ventral cord motor neurons and body muscles does not depend critically on the correct axon pathfinding of motor neurons and appears to be initiated by motor neurons responding to signals from muscle arms (Hedgecock et al., 1990). On the other hand, mechanosensory and SAB neurons may form synapses onto their targets only after they are guided to the target regions. The different mutant phenotypes in mechanosensory and motor neurons may reflect the differences in how synapses are formed in different neurons or may indicate that *rpm-1* has different functions in different neurons.

Phenotypic Comparison of *rpm-1* Mutants with *Drosophila* Mutants

Several *Drosophila* mutants exhibit alterations in presynaptic structures. In *dlg, Fas II* single, and *eag; Shaker* double mutants, the number of presynaptic active zones within a single bouton is increased (Jia et al., 1993; Budnik et al., 1996; Thomas et al., 1997). These extra active zones appear to be the result of increased synaptic activity. *rpm-1* mutants are normal in movement and other visible behaviors, and synaptic transmission appears to not be affected because they exhibit normal sensitivity to the cholinergic synaptic transmission inhibitor aldicarb. Based on the behaviors, the extra presynaptic active zones in *rpm-1* mutants may not be caused by increased synaptic activity.

In *Drosophila hiw* mutants, the total number of synaptic boutons for each glutamatergic NMJ is increased, but the presynaptic ultrastructure in a single bouton is largely normal (Wan et al., 2000). In *rpm-1* mutants, although multiple active zones are present in the same presynaptic varicosity, each active zone has docked vesicles and appears to oppose different muscle arms. The difference in mutant phenotypes between *hiw* and *rpm-1* may be a reflection of differences in how NMJs are formed in *C. elegans* and *Drosophila*. *C. elegans* NMJs do not have boutons, and presynaptic varicosities cannot sprout, whereas *Drosophila* motor axons seek out muscles and form numerous boutons once contact is established. The oversprouting synaptic boutons in *hiw* mutants and the large synapses with multiple active zones in *rpm-1* could thus be mechanistically equivalent defects.

The unusual electron-dense debris in some *rpm-1* mutant synapses is reminiscent of that seen in *Drosphila* CSP mutants, in which synapses undergo premature death when synaptic transmission is blocked (Zinsmaier et al., 1994). However, we observed no changes in the shape and the number of synaptic GFP puncta in *rpm-1* mutants over a few days. This observation, together with the early *rpm-1* temperature-sensitive period and normal behaviors of *rpm-1* mutants, suggests that the underdeveloped presynaptic terminals in *rpm-1* mutants is likely the result of failure in the initial formation, not in the maintenance, of synapses.

rpm-1 Function in NMJ Formation

C. elegans NMJs are formed en passant between neuronal processes and adjacent specialized muscle processes known as muscle arms (White et al., 1976, 1986). Muscle arms appear to actively seek out nerve processes by an unknown chemoattractive signaling mechanism (Hedgecock et al., 1990). How the regular spacing of NMJs is achieved is not known. Because all body wall muscles in *C. elegans* are coupled through electrical synapses (White et al., 1986), the total number and the site of NMJs may not be critical for muscle activation.

It is possible that *rpm-1* may regulate the spacing of presynaptic varicosities. In the absence of *rpm-1*, NMJs are formed at random. The closely positioned NMJs may fuse, giving rise to an overdeveloped appearance. Some of the unfused individual NMJs may degenerate or may not develop fully because the fused large synapses provide sufficient innervation to muscles (see below). RPM-1 may do so either by defining the optimal regions along the nerve process for forming presynaptic terminals or by preventing presynaptic terminals from fusion.

Alternatively, *rpm-1* may function to restrict the development of presynaptic terminals by preventing the formation of excess presynaptic structures so that only one presynaptic active zone is formed within a presynaptic varicosity. In the absence of *rpm-1*, a rudimentary presynaptic terminal would develop continuously, resulting in a large synapse with multiple presynaptic active zones. Because formation of NMJs is not simultaneous, and body muscle activation can be sustained by input from these synapses, any later formed NMJs are not needed and hence degenerate, resulting in the apparently underdeveloped presynaptic terminals in *rpm-1* mutants. The wild-type locomotion of *rpm-1* mutants shows that the abnormal large synapses are functional. This model would be consistent with studies of vertebrate cholinergic NMJs in which a rudimentary synaptic structure is first formed when the nerve terminals reach the muscle targets, and the final shape of NMJ is achieved through cross-talk between muscles and nerve endings (Sanes and Lichtman, 1999). A similar feedback regulatory mechanism may also exist in NMJ formation in *C. elegans*. Because all body wall muscles are electrically coupled, such feedback regulation may take place in the form of adjusting total numbers of NMJs to maintain a steady level of innervation to muscles.

rpm-1 Signaling

RPM-1, HIW, and Pam show significant similarity in overall protein structure and within specific domains. We show that RPM-1 is not associated with synaptic vesicles but localizes in presynaptic regions and functions presynaptically. HIW is found in the periactive zone at presynaptic terminals (Wan et al., 2000). Pam binds Myc and is found in the nucleus of tissue culture cells (Guo et al., 1998), but its in vivo localization is not known. All three proteins contain a domain that is moderately related to RCC1. Our analysis of the RPM-1::H778A transgene shows that this domain is required for RPM-1 function. RCC1 is a GEF for the Ran GTPase and regulates nuclear transport (Bischoff and Ponstingl, 1991). The mammalian protein p619, which bears an RCC1-like domain, can regulate several GTPases, including Ran, Arf, and Rab (Rosa et al., 1996). The promiscuous GEF specificity of RCC1-like domains and the synaptic localization of RPM-1 suggest that *rpm-1* is unlikely to activate the *C. elegans* Ran.

RPM-1 is likely to regulate protein complex formation at the presynaptic terminal. The C termini of RPM-1, HIW, and Pam contain a RING-H2 zinc finger, a subclass of the zinc finger family (Borden and Freemont, 1996). The RING-H2 finger in the yeast pheromone response protein STE5 mediates oligoprotein complex formation (Inouye et al., 1997). The RING-H2 fingers in the mammalian tyrosine kinase regulator Cbl and yeast cell cycle regulators Hrt1 and Cdc53 act as an E2-dependent ubiquitin ligase (Joazeiro et al., 1999; Seol et al., 1999). The large size of RPM-1 would enable it to act as a scaffold for a multiprotein complex, and a function in protein degradation would be consistent with a role in restricting the formation or arrangement of presynaptic structures. Further analysis of the biochemical activity of RPM-1 and identification of its interaction partners will shed light on the mechanisms underlying the development of presynaptic terminals.

Experimental Procedures

Strains and Genetics

C. elegans was grown on NGM plates as described (Brenner, 1974). *ju23*, *ju24*, *ju33*, *ju41*, *ju44*, and *ju48* mutations of *rpm-1* were isolated at 22.5°C from *sem-4(n1376); juIs1* animals treated with ethyl methanesulfonate and shown to be allelic by mapping and noncomplementation test. Briefly, F2 progeny from ~5000 mutagenized haploid genomes were examined for the expression of *juIs1* under Nomaski fluorescence microscope. Animals that had abnormal patterns of the GFP puncta were recovered. *rpm-1* was mapped to *dpy-11 unc-42* on chromosome V based on the following data: from *rpm-1(ju23)/dpy-11(e224)unc-42(e270)* animals, 15 of 44 Unc non-Dpy recombinants and 24 of 28 Dpy non-Unc animals segregated *rpm-1*; from *rpm-1(ju23)/dpy-11(e1180)mom-2(or42)* animals, all 6 Dpy non-Mom recombinants segregated *rpm-1*. *rpm-1* is uncovered by deficiencies *mDf1, stDf29*, and *stDf47* but not by *nDf31* and *eDf1*. *oxIs22* contains an integrated transgene of the functional UNC-49B::GFP marker. *juIs330* contains an integrated array of [P *unc-25*SYD-2(+); pRF4] (Zhen and Jin, 1999).

Cloning of *rpm-1*

Cosmids were from the Sanger Centre, Hinxton, UK. DNA preparation and subcloning were performed following standard procedures (Sambrook et al., 1989). pCZ160 contained an 18 kb PstI-SalI fragment from cosmid C01B7 and rescued *rpm-1* fully. pCZ161 was generated by inserting a 1.0 kb PstI fragment containing GFP (provided by A. Fire) into pCZ160; however, GFP could only be detected by immunofluorescent analysis using anti-GFP antibodies. pCZ163 was generated by digesting pCZ160 with SpII and blunt ending the site with Klenow. pCZ168, pCZ169, and pCZ170 were generated from pCZ160 by simple digestion and religation. The sequences of cDNAs yk349b12, yk397f1, and yk194f8, isolated by *C. elegans* EST database, confirmed the predicted *rpm-1* gene structure between amino acid 2850 and 3′UTR; and the region between amino acid 1775 and amino acid 2466, which spans the duplication breakpoint, was confirmed by RT-PCR products. The $P_{unc\text{-}25}$*rpm-1* construct was made by inserting a 1.2 kb *unc-25* promoter in front of the predicted initiation ATG of *rpm-1* genomic DNA.

Germline transformation was performed following standard procedures using 20–50 ng/μl *rpm-1* DNA and 50 ng/μl pRF4 coinjection marker (Mello et al., 1991). Integrants of RPM-1::GFP (*juIs58*) were obtained by an x-ray-induced mutagenesis of transgenic lines containing *juEx91* [pCZ161; pRF4] and were backcrossed multiple times before use.

Partial Duplication of *rpm-1*

We realized that part of *rpm-1* might be duplicated because the G6224A alteration in the *ju23* mutation was always accompanied by the wild-type nucleotide. The partial sequences of cDNA yk238a8 generated by the *C. elegans* EST database match the potential duplicated region (Y. Kohara, personal communication). Upon reexamining the 3′ end sequences of this cDNA, we found that the last 76 nucleotides of this cDNA identified sequences from the cosmid K06C4, which lies to the right of cosmid C01B7 on the same chromosome. The *C. elegans* Genome Consortium reexamined the sequences of this region and suggested that a minimal 42 kb tandem chromosomal duplication resides to the right of the cosmid C01B7 (Schaefer et al., 2000; J. Spieth, personal communication). This duplication includes 9 kb genomic sequences of the 18 kb (PstI-SalI) *rpm-1* rescuing fragment, and the endpoint of the duplication corresponds to nucleotide 9278 (the 5′ PstI as 1), which is right after the residue Ala-1952 (Figure 4). The presence of cDNA yk238a8 suggests that the partial copy of *rpm-1* is transcribed; however, the exact identity of this gene is unknown.

Site-Directed Mutagenesis

The RPM-1::H778A point mutation was generated following standard procedures using oligonucleotides on single stranded DNA template (Zoller and Smith, 1987). Briefly, a 1.1 kb XhoI-NheI fragment of *rpm-1* genomic DNA was cloned into pBluescript (Stratagen), and single stranded DNA was prepared. An oligonucleotide (5′-GTAAGCTGTGGAAATTTTGCCACAGTACTTCTTGCATCT-3′) was annealed with the single stranded DNA to mutate His-778 to alanine. The sequences of the mutated fragment were determined. A SacI-NcoI fragment containing the mutation then replaced the corresponding fragment in pCZ160.

Identification of *rpm-1* Mutations

rpm-1 genomic DNA, including all exons and exon–intron junctions, was amplified from *rpm-1* mutant and wild-type animals. DNA sequences were determined using ^{33}P-labeled primers and the *fmol* sequencing kit (Promega). All mutant lesions were confirmed on both strands from DNAs prepared in independent PCRs. Sequences of primers and specific nucleotide changes are available upon request.

GFP and Immunocytochemistry Analysis

The DNA for the C-terminal 260 amino acid (M3232–I3492) of RPM-1 was generated by PCR and fused in-frame with glutathione S-transferase in pGEX1λT (Pharmacia). The RPM-1-GST fusion proteins were purified as inclusion bodies and immunized in rats (Harlow and Lane, 1999). Anti-RPM-1 antisera (Cocalico) were affinity purified against GST and RPM-1-GST that were immobilized on nitrocellulose membrane. Whole-mount immunofluorescent staining was performed on animals fixed in 1% paraformaldehyde following the protocol as described (Finney and Ruvkun, 1990). Double immunofluorescent staining with anti-SYD-2 and anti-GFP antibodies was performed as described (Zhen and Jin, 1999). Cy5- or FITC-conjugated secondary antibodies (Cappel) were used at 0.375 μg/μl. GFP was observed using an HQ-FITC filter (Chroma) under the 63× objective of a Zeiss Axioskop fluorescence microscope. Images of immunocytochemistry samples were collected using a Leica confocal microscope.

Mosaic Analysis

Strains containing *rpm-1(ju23); juIs1; Ex*[C01B7 *(rpm-1)*+ SUR-5::GFP] were generated by injecting *rpm-1(ju23); juIs1* animals with 20 ng/μl C01B7 cosmid DNA and 50 ng/μl SUR-5::GFP. SUR-5::GFP is expressed in all somatic cell nuclei (Yochem et al., 1998). Mosaic animals that retained *rpm-1(+)* in AB but not P_1 lineages expressed SUR-5::GFP in neurons but not muscles; mosaic animals that retained *rpm-1(+)* in P_1 but not AB lineages expressed SUR-5::GFP in muscles but not neurons.

EM Fixation and Analysis

CZ333 *juIs1*, CZ454 *rpm-1(ju41); juIs1*, CZ455 *rpm-1(ju44); juIs1* young adult animals were fixed in parallel using glutaraldehyde and osmium as described (Jin et al., 1999). Fixed worms were first cut with glass knives at the posterior pharyngeal bulb. Regions between the posterior pharyngeal bulb and the vulva were cut with diamond knives, and 200–400 serial thin sections of 50–60 nm thickness were collected for each sample. The ventral and/or dorsal nerve cords

were photographed and examined. Chemical synapses were identified by the accumulation of synaptic vesicles and the appearance of darkly stained active zones. GABAergic NMJs were identified as synapses made by DD/VD neurons to muscle arms. Cholinergic NMJs were identified as dyadic synapses to both DD or VD neurons and muscles (White et al., 1976, 1986). Neuron–neuron synapses include those that do not have muscle arms as postsynaptic partners. Presynaptic active zones were recognized as electron-dense membrane thickenings surrounded by synaptic vesicles in presynaptic varicosities. One to three animals of each genotype were examined.

Temperature Shift Experiments

For upshift experiments, 20–40 *ju44; juIs1* worms that had been maintained at 15°C were upshifted to 25°C at different developmental stages, grown to adulthood, and examined for $P_{unc\text{-}25}$SNB-1::GFP phenotype; vice versa for downshift experiments. Animals that had more than eight fluorescent puncta of normal size per VD neuron were scored as wild-type; animals that had two or more large fluorescent puncta per VD neuron, as mutant. Developmental stages were estimated from the time after lysing adults (time 0) and, in some cases, confirmed by examining larval stage–specific landmarks. Specific time points (hours at 25°C/15°C) are 7/15 for early L1s, 13/24 for mid-L1s, 19/39 for late L1s and early L2s, 23/52 for mid-L2s, 28/63 for late L2s and early L3s, 34/68 for mid-L3s, 39/75 for later L3s and early L4s, and 43/90 for L4s.

Acknowledgments

We thank M. Nonet for SNB-1::GFP DNA and anti-SNT-1 antibodies; G. Crump and C. Bargmann for *rpm-1* alleles; M. Han for SUR-5::GFP; Y. Kohara for *rpm-1* cDNAs; the *C. elegans* Genome Consortium for the sequences and cosmid DNAs used in this report; A. Fire for GFP vectors; J.-P. Bessereau for integrating UNC-49B::GFP; D. Hall for his advice on the EM analysis; J. White for unpublished EM observations; H. Wan and C. Goodman for communicating unpublished results and discussions; A. Schaefer and M. Nonet for sharing data on the duplication and unpublished results; and A. Chisholm, E. Jorgensen, R. Baran, D. Byrd, I. Chin-Sang, and members of the Jin and Chisholm laboratories for comments on the manuscript. Some of the strains used here were obtained from the Caenorhabditis Genetics Center, which is supported by the National Institutes of Health. M. Z. is supported by a long-term Human Frontier Science Fellowship. Y. J. is an Alfred P. Sloan research fellow. This work is supported by National Institutes of Health grant NS-35546 to Y. J.

Received April 11, 2000; revised April 26, 2000.

References

Azuma, Y., Seino, H., Seki, T., Uzawa, S., Klebe, C., Ohba, T., Wittinghofer, A., Hayashi, N., and Nishimoto, T. (1996). Conserved histidine residues of RCC1 are essential for nucleotide exchange on Ran. J. Biochem. *120*, 82–91.

Bamber, B.A., Beg, A.A., Twyman, R.E., and Jorgensen, E.M. (1999). The *Caenorhabditis elegans unc-49* locus encodes multiple subunits of a heteromultimeric GABA receptor. J. Neurosci. *19*, 5348–5359.

Bischoff, F.R., and Ponstingl, H. (1991). Catalysis of guanine nucleotide exchange on Ran by the mitotic regulator RCC1. Nature *354*, 80–82.

Borden, K.L., and Freemont, P.S. (1996). The RING finger domain: a recent example of a sequence-structure family. Curr. Opin. Struct. Biol. *6*, 395–401.

Brenner, S. (1974). The genetics of *Caenorhabditis elegans*. Genetics *77*, 71–94.

Budnik, V., Koh, Y.H., Guan, B., Hartmann, B., Hough, C., Woods, D., and Gorczyca, M. (1996). Regulation of synapse structure and function by the Drosophila tumor suppressor gene *dlg*. Neuron *17*, 627–640.

Burns, M.E., and Augustine, G.J. (1995). Synaptic structure and function: dynamic organization yields architectural precision. Cell *83*, 187–194.

Chalfie, M., Tu, Y., Euskirchen, G., Ward, W.W., and Prasher, D.C. (1994). Green fluorescent protein as a marker for gene expression. Science *263*, 802–805.

Chen, H.J., Rojas-Soto, M., Oguni, A., and Kennedy, M.B. (1998). A synaptic Ras-GTPase activating protein (p135 SynGAP) inhibited by CaM kinase II. Neuron *20*, 895–904.

Cho, K.O., Hunt, C.A., and Kennedy, M.B. (1992). The rat brain postsynaptic density fraction contains a homolog of the Drosophila discs-large tumor suppressor protein. Neuron *9*, 929–942.

Fenster, S.D., Chung, W.J., Zhai, R., Cases-Langhoff, C., Voss, B., Garner, A.M., Kaempf, U., Kindler, S., Gundelfinger, E.D., and Garner, C.C. (2000). Piccolo, presynaptic zinc finger protein structurally related to Bassoon. Neuron *25*, 203–214.

Finney, M., and Ruvkun, G. (1990). The *unc-86* gene product couples cell lineage and cell identity in *C. elegans*. Cell *63*, 895–905.

Gramates, S.L., and Budnik, V. (1999). Assembly and maturation of the Drosophila larval neuromuscular junction. Int. Rev. Neurobiol. *43*, 93–117.

Guo, Q., Xie, J., Dang, C.V., Liu, E.T., and Bishop, J.M. (1998). Identification of a large Myc-binding protein that contains RCC1-like repeats. Proc. Natl. Acad. Sci. USA *95*, 9172–9177.

Hall, D.H., and Hedgecock, E.M. (1991). Kinesin-related gene *unc-104* is required for axonal transport of synaptic vesicles in *C. elegans*. Cell *65*, 837–847.

Hall, Z.W., and Sanes, J.R. (1993). Synaptic structure and development: the neuromuscular junction. Cell *72 (suppl.)*, 99–121.

Hallam, S.J., and Jin, Y. (1998). *lin-14* regulates the timing of synaptic remodeling in *Caenorhabditis elegans*. Nature *395*, 78–82.

Harlow, E., and Lane, D. (1999). Using Antibodies: A Laboratory Manual (Cold Spring Harbor, NY: Cold Spring Harbor Laboratory Press).

Hedgecock, E.M., Culotti, J.G., and Hall, D.H. (1990). The *unc-5*, *unc-6*, and *unc-40* genes guide circumferential migrations of pioneer axons and mesodermal cells on the epidermis in *C. elegans*. Neuron *4*, 61–85.

Heuser, J.E., and Reese, T.S. (1977). Structure of the synapse. In The Handbook of Physiology, The Nervous System, Volume One, E. Kandel, ed. (Baltimore: Williams and Wilkins), pp. 261–294.

Hirokawa, N., Sobue, K., Kanda, K., Harada, A., and Yorifuji, H. (1989). The cytoskeletal architecture of the presynaptic terminal and molecular structure of synapsin 1. J. Cell Biol. *108*, 111–126.

Inouye, C., Dhillon, N., and Thorner, J. (1997). Ste5 RING-H2 domain: role in Ste4-promoted oligomerization for yeast pheromone signaling. Science *278*, 103–106.

Jia, X.X., Gorczyca, M., and Budnik, V. (1993). Ultrastructure of neuromuscular junctions in Drosophila: comparison of wild type and mutants with increased excitability. J. Neurobiol. *24*, 1025–1044.

Jin, Y., Jorgensen, E., Hartwieg, E., and Horvitz, H.R. (1999). The *Caenorhabditis elegans* gene *unc-25* encodes glutamic acid decarboxylase and is required for synaptic transmission but not synaptic development. J. Neurosci. *19*, 539–548.

Joazeiro, C.A., Wing, S.S., Huang, H., Leverson, J.D., Hunter, T., and Liu, Y.C. (1999). The tyrosine kinase negative regulator c-Cbl as a RING-type, E2-dependent ubiquitin-protein ligase. Science *286*, 309–312.

Jorgensen, E.M., and Rankin, C. (1997). Neural Plasticity. In *C. elegans* II, D.L. Riddle et al., eds. (Cold Spring Harbor, NY: Cold Spring Harbor Laboratory Press), pp. 769–790.

Jorgensen, E.M., Hartwieg, E., Schuske, K., Nonet, M.L., Jin, Y., and Horvitz, H.R. (1995). Defective recycling of synaptic vesicles in synaptotagmin mutants of *Caenorhabditis elegans*. Nature *378*, 196–199.

Kennedy, M.B., Bennett, M.K., and Erondu, N.E. (1983). Biochemical and immunochemical evidence that the "major postsynaptic density protein" is a subunit of a calmodulin-dependent protein kinase. Proc. Natl. Acad. Sci. USA *80*, 7357–7361.

Kim, J.H., Liao, D., Lau, L.F., and Huganir, R.L. (1998). SynGAP: a synaptic RasGAP that associates with the PSD-95/SAP90 protein family. Neuron *20*, 683–691.

Kistner, U., Wenzel, B.M., Veh, R.W., Cases-Langhoff, C., Garner, A.M., Appeltauer, U., Voss, B., Gundelfinger, E.D., and Garner, C.C. (1993). SAP90, a rat presynaptic protein related to the product of the Drosophila tumor suppressor gene dlg-A. J. Biol. Chem. *268*, 4580–4583.

Koh, Y.H., Popova, E., Thomas, U., Griffith, L.C., and Budnik, V. (1999). Regulation of DLG localization at synapses by CaMKII-dependent phosphorylation. Cell *98*, 353–363.

Landis, D.M., Hall, A.K., Weinstein, L.A., and Reese, T.S. (1988). The organization of cytoplasm at the presynaptic active zone of a central nervous system synapse. Neuron *1*, 201–209.

Leung-Hagesteijn, C., Spence, A.M., Stern, B.D., Zhou, Y., Su, M.-W., Hedgecock, E.M., and Culotti, J.G. (1992). UNC-5, a transmembrane protein with immunoglobulin and thrombospondin type 1 domains, guides cells and pioneer axon migrations in *C. elegans*. Cell *71*, 289–299.

Mello, C.C., Kramer, J.M., Stinchcomb, D., and Ambros, V. (1991). Efficient gene transfer in C. elegans: extrachromosomal maintenance and integration of transforming sequences. EMBO J. *10*, 3959–3970.

Nguyen, M., Alfonso, A., Johnson, C.D., and Rand, J.B. (1995). *Caenorhabditis elegans* mutants resistant to inhibitors of acetylcholinesterase. Genetics *140*, 527–535.

Nonet, M.L. (1999). Visualization of synaptic specializations in live *C. elegans* with synaptic vesicle protein–GFP fusions. J. Neurosci. Methods *89*, 33–40.

Nonet, M.L., Grundahl, K., Meyer, B.J., and Rand, J.B. (1993). Synaptic function is impaired but not eliminated in *C. elegans* mutants lacking synaptotagmin. Cell *73*, 1291–1305.

Pieribone, V.A., Shupliakov, O., Brodin, L., Hilfiker-Rothenfluh, S., Czernik, A.J., and Greengard, P. (1995). Distinct pools of synaptic vesicles in neurotransmitter release. Nature *375*, 493–497.

Rand, J.B., and Nonet, M.L. (1997). Synaptic transmission. In *C. elegans* II, D.L. Riddle et al., eds. (Cold Spring Harbor, NY: Cold Spring Harbor Laboratory Press), pp. 611–643.

Renault, L., Nassar, N., Vetter, I., Becker, J., Klebe, C., Roth, M., and Wittinghofer, A. (1998). The 1.7 A crystal structure of the regulator of chromosome condensation (RCC1) reveals a seven-bladed propeller. Nature *392*, 97–101.

Rosa, J.L., Casaroli-Marano, R.P., Buckler, A.J., Vilaro, S., and Barbacid, M. (1996). p619, a giant protein related to the chromosome condensation regulator RCC1, stimulates guanine nucleotide exchange on ARF1 and Rab proteins. EMBO J. *15*, 4262–4273.

Rosahl, T.W., Spillane, D., Missler, M., Herz, J., Selig, D.K., Wolff, J.R., Hammer, R.E., Malenka, R.C., and Südhof, T.C. (1995). Essential functions of synapsins I and II in synaptic vesicle regulation. Nature *375*, 488–493.

Sambrook, J., Fritsch, E.F., and Maniatis, T. (1989). Molecular Cloning: A Laboratory Manual (Cold Spring Harbor, NY: Cold Spring Harbor Labortatory Press).

Sanes, J.R., and Lichtman, J.W. (1999). Development of the vertebrate neuromuscular junction. Annu. Rev. Neurosci. *22*, 389–442.

Schaefer, A.M., Hadwiger, G.D., and Nonet, M.L. (2000). *rpm-1*, a conserved neuronal gene that regulates targeting and synaptogenesis in *C. elegans*. Neuron *26*, this issue, 345–356.

Seol, J.H., Feldman, R.M., Zachariae, W., Shevchenko, A., Correll, C.C., Lyapina, S., Chi, Y., Galova, M., Claypool, J., Sandmeyer, S., et al. (1999). Cdc53/cullin and the essential Hrt1 RING-H2 subunit of SCF define a ubiquitin ligase module that activates the E2 enzyme Cdc34. Genes Dev. *13*, 1614–1626.

Sulston, J.E. (1976). Post-embryonic development in the ventral cord of *C. elegans*. Philos. Trans. R. Soc. Lond. B Biol. Sci. *275*, 287–297.

Thomas, U., Kim, E., Kuhlendahl, S., Koh, Y., Gundelfinger, E., Sheng, M., Garner, C., and Budnik, V. (1997). Synaptic clustering of the cell adhesion molecule Fasciclin II by Discs-large and its role in the regulation of presynaptic structure. Neuron *19*, 787–799.

tom Dieck, S., Sanmarti-Vila, L., Langnaese, K., Richter, K., Kindler, S., Soyke, A., Wex, H., Smalla, K.-H., Kampf, U.M., Franzer, J.-T., et al. (1998). Bassoon, a novel zinc-finger CAG/glutamine-repeat protein selectively localized at the active zone of presynaptic nerve termini. J. Cell Biol. *142*, 499–509.

Wan, H.I., DiAntonio, A., Fetter, R.D., Bergstrom, K., Strauss, R., and Goodman, C.S. (2000). Highwire regulates synaptic growth in *Drosophila*. Neuron *26*, this issue, 313–329.

Wang, X., Kibschull, M., Laue, M.M., Lichte, B., Petrasch-Parwez, E., and Kilimann, M.W. (1999). Aczonin, a 550-kD putative scaffolding protein of presynaptic active zones, shares homology regions with rim and bassoon and binds profilin. J. Cell Biol. *147*, 151–162.

Wang, Y., Okamoto, M., Schmitz, F., Hofmann, K., and Südhof, T.C. (1997). Rim is a putative Rab3 effector in regulating synaptic-vesicle fusion. Nature *388*, 593–598.

White, J.G., Southgate, E., Thomson, J.N., and Brenner, S. (1976). The structure of the ventral nerve cord of *Caenorhabditis elegans*. Philos. Trans. R. Soc. Lond. B Biol. Sci. *275*, 327–348.

White, J.G., Southgate, E., Thomson, J.N., and Brenner, S. (1986). The structure of the nervous system of the nematode *Caenorhabditis elegans*. Philos. Trans. R. Soc. Lond. B Biol. Sci. *314*, 1–340.

Woods, D.F., and Bryant, P.J. (1991). The discs-large tumor suppressor gene of Drosophila encodes a guanylate kinase homolog localized at septate junctions. Cell *66*, 451–464.

Yochem, J., Gu, T., and Han, M. (1998). A new marker for mosaic analysis in *Caenorhabditis elegans* indicates a fusion between hyp6 and hyp7, two major components of the hypodermis. Genetics *149*, 1323–1334.

Zhen, M., and Jin, Y. (1999). The liprin protein SYD-2 regulates the differentiation of presynaptic termini in *C. elegans*. Nature *401*, 371–375.

Ziff, E.B. (1997). Enlightening the postsynaptic density. Neuron *19*, 1163–1174.

Zinsmaier, K.E., Eberle, K.K., Buchner, E., Walter, N., and Benzer, S. (1994). Paralysis and early death in cysteine string protein mutants of Drosophila. Science *263*, 977–980.

Zoller, M.J., and Smith, M. (1987). Oligonucleotide-directed mutagenesis: a simple method using two oligonucleotide primers and a single-stranded DNA template. Methods Enzymol. *154*, 329–350.